IDENTIFICATION OF SERIES RESISTANCE FROM THE MEASURED PV PANEL ELECTRICAL CHARACTERISTICS

H. Kalliojärvi-Viljakainen*, G. Spagnuolo**, S. Valkealahti*
*Tampere University, Tampere, Finland
**University of Salerno, Salerno, Italy

ABSTRACT: The condition of a solar PV panel can be evaluated by its measured electrical characteristics. The single-diode model parameters extracted from a measured current-voltage curve may indicate the possible presence of degradation. Aging of PV cells is a common source of degradation and manifests itself typically in increased series resistance values, causing a decline in the voltage characteristics of a PV panel. However, the current and voltage characteristics of a PV panel change considerably with changing environmental conditions, especially with changing irradiance and temperature. Accordingly, the single diode model parameter values change along variations in the surrounding environmental conditions, making the comparison of any two distinct current-voltage curves measured in outdoor conditions difficult. This gives a reason for converting the identified single diode model parameters of a measured curve from actual operating conditions to common reference conditions. In this light, we study the relation between the PV panel voltage and series resistance under different environmental conditions. We also investigate the feasibility of parameter reversion back to standard test conditions.
Keywords: PV panel, aging, series resistance, evaluation, degradation

1 INTRODUCTION

Among the various degradation modes occurring in photovoltaic (PV) systems, aging of PV cells is responsible for a major part of performance problems on long term. Usually aging effects are observed as increased series resistance levels. Unfortunately, there is no reliable and well assessed way for measuring this parameter and a mathematical identification procedure is mandatory. Many of the recent works base their parameter identification procedure on Lambert W function by which the implicit equation of the PV single diode model can be explicitly solved. The topic is richly encompassed in [1] and the explicit formulae enable the online diagnosis of PV systems. Recent contributions to PV panel parameter identification and aging detection rely on the Lambert W function [2], [3]. They exploit the dependence of certain single diode model parameters on outdoor conditions and replace them by irradiance and temperature in the parameter extraction procedure. The series-parallel ratio, an index initially introduced in the simplified four-parameter model applying also Lambert W function [4], is utilized as an indicator in aging detection in [2].

Although several indicators presented in literature are capable of detecting aging, the quantification of this phenomenon is not straightforward. A model-based indicator for quantification of series resistance increment was originally developed in the work by [5] and later improved by [6] via the parameter identification method [7]. In there, the Lambert W function serves as the tool for parameter identification.

To avoid complicated mathematical formulae, a feasible option is to retain the implicit single diode equation and solve the parameters via an iterative fitting procedure. One very popular approach is the one introduced by [8]. Such methodology, even though not easily applicable online, provides a valuable complementary tool for the offline part of diagnosis due to its good accuracy and simple implementation by MATLAB or some other calculating program. The state-of-the-art review article [9] and the book [1], among others, provide a deeper insight on different parameter extraction techniques.

The single diode model parameters fluctuate by irradiance and temperature conditions as well. So degradation is not the only possible origin of parameter drift. In this light, an individual series resistance value is rather useless as itself it is not directly comparable with the value extracted from another current-voltage curve measured in some other environmental conditions. To enable the comparison of two curves, one should convert their characteristics to some common reference condition. There are two possibilities: either to convert the current and voltage at the critical points and fit a curve through them or to apply conversion formulas directly to the identified parameters. The former approach is applied e.g. in [10], [11]. However, the knowledge of case-specific empirical coefficients is required. For the latter approach, one widely used procedure is [12], providing expressions for the single diode model parameters as functions of a reference value and environmental conditions. A very similar set of conversion formulas is given by [8]. The difference between [12] and [8] lies in the expression of saturation current. The single diode model was tuned in [13] by inserting an additional term to account for thermal effects before converting the parameters.

Series resistance increments affect crucially the operating voltage of the PV panel. The effect is most visible in the vicinity of the maximum power point (mpp) [14]. Since changes in series resistance have an impact on the slope of the *I-U* curve also near the open circuit (OC) condition, slight changes in open circuit voltage occur too [10,15]. These facts may well be used in diagnosis, as shown by [2]. In the beginning of the life span of a PV panel, one can capture the reference values for voltage characteristics and series resistance. For the conversion of series resistance and open circuit voltage, widely validated formulas from literature can be used. The reversion of the maximum power point voltage is more challenging and might require the joint use of semi-empirical models and case-specific experimental measurements.

The present work focuses on series resistance identification in light of [2] and [8]. For doing that we consider the relation between voltage characteristics and series resistance levels under different environmental conditions and convert the obtained single diode model parameters obtained via [8] to reference conditions and finally evaluate the overall performance of the conversion

procedure.

The paper is organized as follows. Section 2 is dedicated for reviewing the requisite preliminaries, including the formulae used as the starting point. Section 3 represents the experimental setup as well as the data utilized in it. Section 4 gathers the results, providing also discussion and criticism on them. The paper is concluded in Section 5.

2 THEORETICAL FRAMEWORK

2.1 Single-diode model

PV cells and panels are modelled by the single diode model providing an equivalent circuit of a PV unit. The model gives the PV output current I as an implicit function of both I and U, the latter of which standing for the PV output voltage, as follows

$$I = I_{ph} - I_o\left(\exp\left(\frac{U+IR_s}{AV_t}\right) - 1\right) - \frac{U+IR_s}{R_h}. \quad (1)$$

The light-generated current I_{ph} represents the electron-hole pairs enabling the flow of the current through the PV cell. The diode saturation current I_o describes the small flow of the minority charge carriers across the p-n junction. The ideality factor A indicates to what extent the diode behaves like an ideal diode. The series resistance R_s and the shunt resistance R_h illustrate the voltage-related and current-related loss mechanisms, respectively. The thermal voltage V_t is calculated as $n_s kT/q$, where k is the Boltzmann constant, n_s is the number of the series-connected PV cells, T is the absolute operating temperature of the panel, and q is the electron charge.

2.2 Obtaining single diode model parameter

Conversion of the single diode model parameter obtained by fitting to PV module nameplate values in standard test conditions (STC), i.e. light spectrum of AM1.5, irradiance G of 1000 W/m^2 and panel operating temperature T of 25 ºC, is done in line with [8] to the actual operating conditions using the following formulae:

$$I_{sc} = I_{sc,STC}\left(1 + K_I(T - T_{STC})\right)\left(\frac{G}{G_{STC}}\right) \quad (2)$$

$$R_s = R_{s,STC} \quad (3)$$

$$I_{ph} = I_{sc}\left(1 + \frac{R_s}{R_h}\right) \quad (4)$$

$$I_o = \frac{I_{sc} - \frac{U_{oc,STC}(1 + K_V(T - T_{STC}))}{R_h}}{exp\left(\frac{U_{oc,STC}(1 + K_V(T - T_{STC}))}{AV_t}\right) - 1}. \quad (5)$$

In there, I_{SC} is the short circuit (SC) current, U_{OC} the open circuit voltage and K_I and K_V stand for the temperature coefficients of the short circuit current and open circuit voltage. These coefficients are obtained via scaling the corresponding temperature coefficients reported in the PV panel datasheet provided by the manufacturer. Originally, A is required to have a fixed value between 1 and 1.5 in [8]. Our choice of 1.3 is a typical value for PV cells fabricated of crystalline silicon and is justified in [16]. To improve the accuracy of the model, an additional equation

$$R_h = R_{h,STC}\left(\frac{G}{G_{STC}}\right) \quad (6)$$

adopted from [12] has been inserted in the collection of the formulae. The values of $R_{h,STC}$ and $R_{s,STC}$ at STC are obtained via an iterative procedure, whose details are explained in [8]. For the PV module considered in this paper, the datasheet values at STC are reported in Table I.

Table I: Datasheet parameter values at STC.

Quantity	Value
$U_{oc,STC}$	33.1 V
$U_{mpp,\,STC}$	25.9 V
$I_{sc,STC}$	8.02 A
$I_{mpp,\,STC}$	7.33 A
K_V	-0.124 V/K
K_I	0.0047 A/K
$R_{s,STC}$	0.33 Ω
$R_{h,STC}$	188 Ω

2.2. Inverse conversion of parameters to STC

Inverse conversion of the Eqs. (2) to (6) back from the environmental conditions during the measurement to STC implies

$$I_{SC,STC} = \frac{I_{SC}}{1 + K_I(T - T_{STC})}\left(\frac{G_{STC}}{G}\right) \quad (7)$$

$$R_{s,STC} = R_s \quad (8)$$

$$R_{h,STC} = R_h\left(\frac{G_{STC}}{G}\right) \quad (9)$$

$$I_{ph,STC} = I_{sc,STC}\left(1 + \frac{R_s}{R_{h,STC}}\right) \quad (10)$$

$$I_{o,STC} = \frac{I_{sc,STC} - \frac{U_{oc,STC}}{R_{h,STC}}}{\exp\left(\frac{U_{oc,STC}}{AV_{t,STC}}\right) - 1}. \quad (11)$$

The open circuit voltage in standard test conditions is approximated via its temperature dependence

$$U_{oc,STC} = \frac{Uoc}{1 + K_V(T - T_{STC})}. \quad (12)$$

3 EXPERIMENTAL SETUP

The experimental measurement data have been taken from the solar PV power research plant located on the rooftop of Tampere University [17]. The plant consists of 69 PV panels (NAPS NP190GKg). The used data have been measured from an individual panel. The irradiance received by the panel was captured by a SP Lite2 sensor and the panel operating temperature was approximated by its backside temperature, measured by a Pt100 sensor.

All the current-voltage curves under investigation were measured during the same week, so any noticeable aging would not happen during such a short time period.

For this reason, we emulated the aging effects artificially. To make evident changes in the series resistance, three different-sized resistors, each in its turn, were connected in series with the PV panel under investigation. The magnitudes of these additional resistances were 0.22, 0.47 and 0.69 Ω each of them representing a different stage of aging. Each such case was investigated on the basis of one hour of measured *I-U* data.

The measurements were performed during summertime in Finland, whence the experimental data have irradiance values as given in Table II and temperature values provided in Table III.

Table II: Irradiance conditions during the *I-U* curve measurements.

$R_{s,add}$ (Ω)	G_{min} (W/m^2)	G_{max} (W/m^2)
0	154	1060
0.22	453	1278
0.47	177	1071
0.69	182	998

Table II: Temperature conditions during the *I-U* curve measurements.

$R_{s,add}$ (Ω)	T_{min} (°C)	T_{max} (°C)
0	28.7	47.9
0.22	41.7	52.6
0.47	42.7	47.2
0.69	47.8	57.2

Table II reveals that irradiance varied from pure diffuse irradiance up to overirradiances caused by the cloud enhancement phenomenon exceeding the nominal clear sky irradiance clearly. Table III reveals that any extremely low or high temperatures were not present, i.e. the temperature range was on medium level.

4 RESULTS

4.1 Behavior of voltage quantities

Many sources, e.g. [3], [4], combine U_{mpp} and U_{oc} into a single number by forming their ratio and it is suggested as a possible aging indicator in [3]. This ratio is simulated in Fig. 1 as a function R_S by using the single diode PV panel characteristics of the Tampere University solar PV power research plant [17] (see Table I). Fig. 1 demonstrated clearly that there is an almost linear dependence between the ratio U_{mpp}/U_{oc} and the series resistance R_S, at least up to five times its STC value.

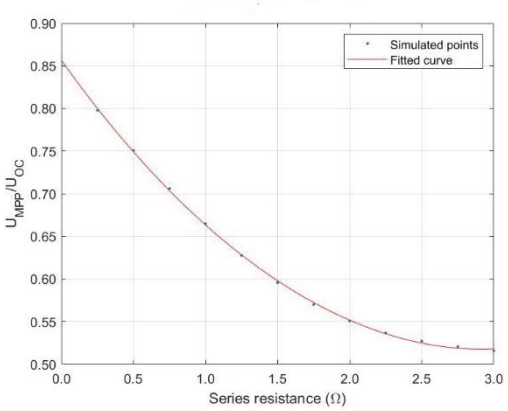

Figure 1: Simulated U_{mpp}/U_{oc} ratio (the dots) of a single PV panel plotted against different series resistance values in STC assuming R_h constant. The fitted line is drawn just to guide the eye.

In addition to aging causing the growth of the resistance and changes in the voltage characteristics, also the outdoor conditions affect strongly on the behavior on the voltage characteristics of the PV panel. When performing diagnosis, the effects of temperature and irradiance need to be filtered out. Growing temperature weakens the performance of the PV panel by lowering the voltage and also irradiance affects the voltage region of the *I-U* curve. Figs. 2 and 3 indicate the vertical shift in the U_{mpp}/U_{oc} versus R_s curve due to temperature effects. This is in line with the well-known linear dependence of voltage on temperature [1]. Temperatures used in the simulations correspond to the minimum and maximum temperatures of the measured *I-U* curves.

Lambert W function is used in the parameter identification process in Fig. 2. It serves as a reference for our method based on Villalva procedure [8] and shown in Fig. 3. In Fig. 3 the measurement noise of the *I-U* data has been smoothed by local polynomial regression (LOESS) method with a span of 0.1 before the identification procedure. It is visible in Figs. 2 and 3 that both the Lambert W function and the Villalva procedure provide quite similar results with the same voltage ratio versus series resistance behavior. Both methods return the series resistances quite accurately with small spread when taking the series resistance of the PV panel (Table I) and of the cables (0.363 Ω) into account in line with theoretical simulations. Both method also have quite similar variation of the voltage ratio. Fig. 4 serves as a warning example on the inaccuracy caused by the use of plain raw measurement data. The measurement noise in the vicinity of open circuit voltage causes a decrease in the voltage ratio and a considerable spread in both measured quantities.

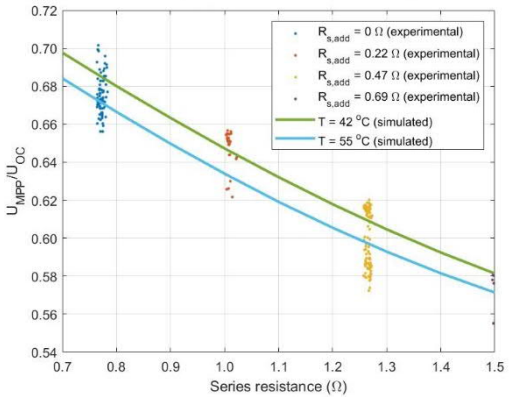

Figure 2: Simulated and experimental U_{mpp}/U_{oc} ratios of a single PV panel *I-U* data plotted against different series resistance values for fixed irradiance of 1 kW/m^2 in the associated temperature range using Lambert W function. Measured points are within a range of 5 W/m^2 from the 1 kW/m^2 irradiance.

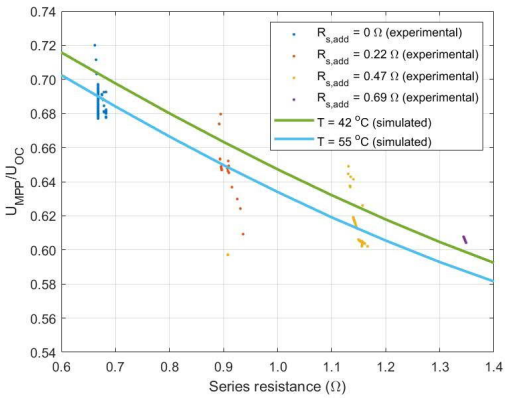

Figure 3: Simulated and experimental U_{mpp}/U_{oc} ratios of a single PV panel, with the measurement noise removed, plotted against different series resistance values for fixed irradiance of 1 kW/m^2 in the associated temperature range using Villalva's method. Measured points are within a range of 5 W/m^2 from the 1 kW/m^2 irradiance.

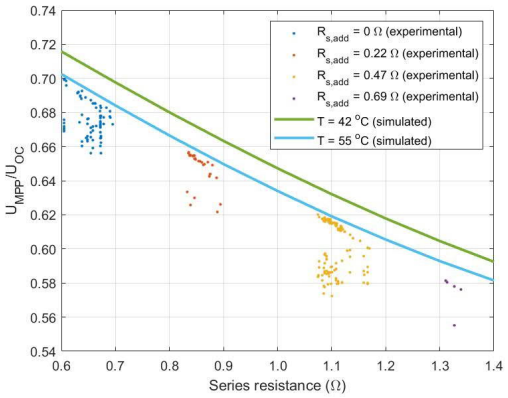

Figure 4: Simulated and experimental U_{mpp}/U_{oc} ratios of a single PV panel extracted directly from the raw *I-U* data plotted against different series resistance values for fixed irradiance of 1 kW/m^2 in the associated temperature range using Villalva's method. Measured points are within a range of 5 W/m^2 from the 1 kW/m^2 irradiance.

The logarithmic dependence of the open circuit voltage on irradiance is a commonly known and theoretically understood phenomenon. Instead, the relation between U_{mpp}/U_{oc} and G is not so obvious. This is clarified by several authors and an overview is given in [1]. The behavior of U_{mpp}/U_{oc} against irradiance has been illustrated in [2] utilizing the Lambert W function for different values of additional series resistance of the PV panel. In comparison, Fig. 5 represents similar results using the method described in [8], including also the simulated curves. The results are in agreement with each other. The decrease of the voltage ratio with increasing series resistance is clearly visible, but the ratio also decreases considerably with increasing irradiance in line with the behavior of the mathematical single diode model.

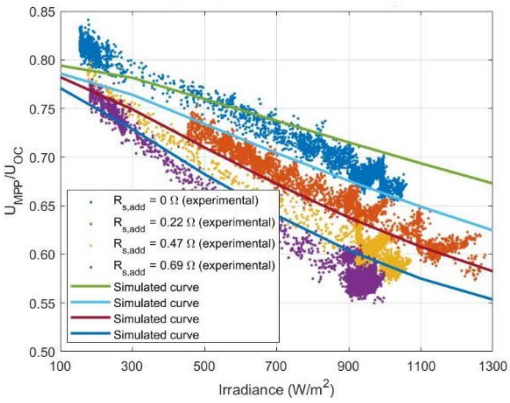

Figure 5: Simulated and experimental (the dots) U_{mpp}/U_{oc} ratios of a single PV panel plotted against irradiance for different series resistance levels.

4.2 Conversion of series resistance to STC

As one aims at distinguishing between parameter drift due to aging and due to environmental conditions, conversion, or even "translation", as it is also named in literature, of the single diode model parameters to reference conditions is mandatory. The entire process includes the conversion of all the five parameters as well as the short circuit current which is needed to calculate the actual set of parameters. Our main focus in this paper is to extract the series resistance parameter values from the measured *I-U* curves and convert them to STC. Fig. 6 shows how the procedure identifies the different additional series resistance from the measured data of one hour.

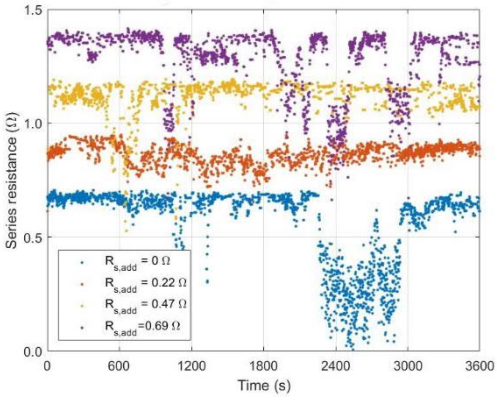

Figure 6: The STC series resistances identified from experimental data against the time of measurement for different additional series resistance.

The used method is able to identify well the additional series resistances having most of the time consistent values (Fig. 6). However, the R_s values drop considerably time to time due to the widely agreed fact that the single diode model fitted to STC conditions fails to perform correctly at low irradiance levels. This phenomenon is shown more clearly in Fig. 7 by plotting the obtained series resistances as a function of irradiance. These results are comparable to [3] and [5], both of which performed the parameter identification procedure via Lambert W function. Figs. 6 and 7 imply that identification of the series resistance values from the measured *I-U* curves to detect aging might

work at least under high irradiance conditions.

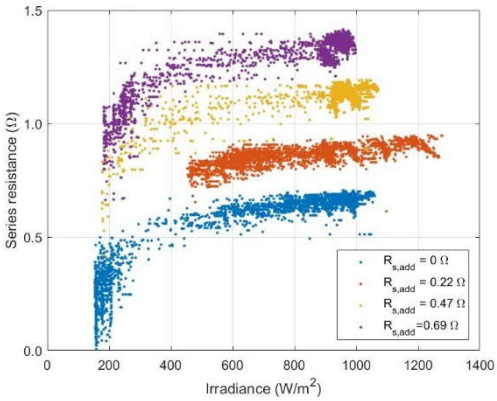

Figure 7: The STC series resistances identified from the experimental data as functions of measured irradiance for different values of additional series resistance.

While the extraction of series resistance is strongly dependent on the irradiance experienced by the PV panel, the identified series resistance has hardly any temperature dependence. This expected result becomes evident from Figs. 8 and 9. Low irradiance values cause a wide spread in the series resistance values (Fig. 8) quite evenly over the whole temperature range. Variation of the series resistance decreases considerably by limiting the irradiance range of the analysed data to high irradiance cases shown in Fig. 9.

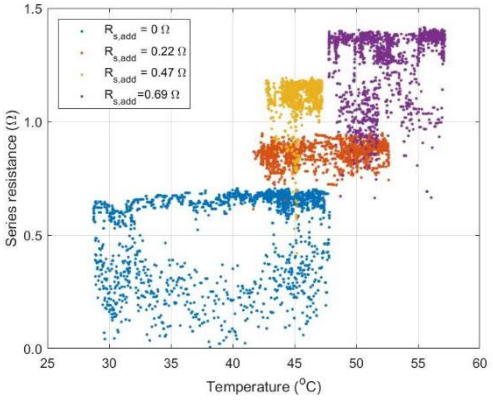

Figure 8: The STC series resistances identified from the experimental data as functions of PV panel operating temperature for different values of additional series resistance in the entire irradiance range.

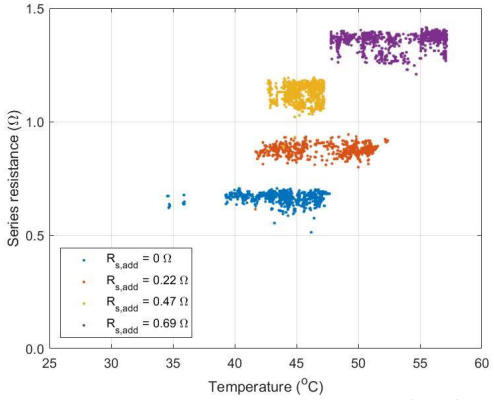

Figure 9: The STC series resistances identified from the experimental data as functions of PV panel operating temperature for different values of additional series resistance at high irradiances between 900 and 1100 W/m^2.

4.3 Conversion of other parameters to STC

Identification and conversion of the short circuit current to STC is needed for calculating the reference values for the photocurrent and the saturation current. The performance of Eq. (7) to convert short circuit current values from the measured data is shown in Fig. 10. It works well at high irradiances, but low irradiances cause drastic peaks from the stable level of the converted $I_{SC,STC}$. This peaking seems to be also related to the malfunctioning of the used procedure at low irradiance levels since the it is based on the single diode model of the electrical behavior of PV cells at STC conditions.

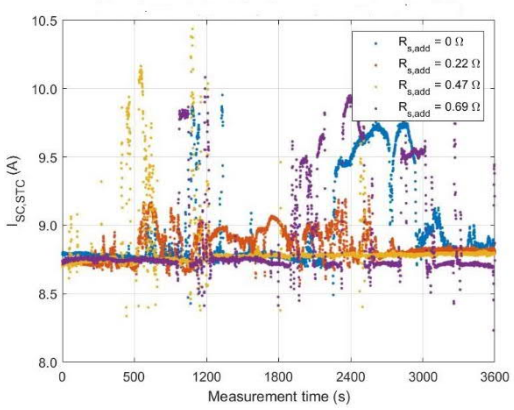

Figure 10: The measured short circuit current converted to STC against the time of measurement for different values of additional series resistance.

The conversion of shunt resistances from the measured *I-U* curves via Eq. (9) is more vague. Fig. 11 depicts the large deviation of the converted shunt resistance values. This is not surprising since the single diode model is not sensitive on the value of the shunt resistance. High quality PV cell typically have very high shunt resistance and, therefore, having a good fit of the one diode model to their electrical characteristics needs to have just a high enough shunt resistance value. On the other hand, an excessively small shunt resistance value converted from the measured *I-U* curve would clearly indicate problems in the PV panel.

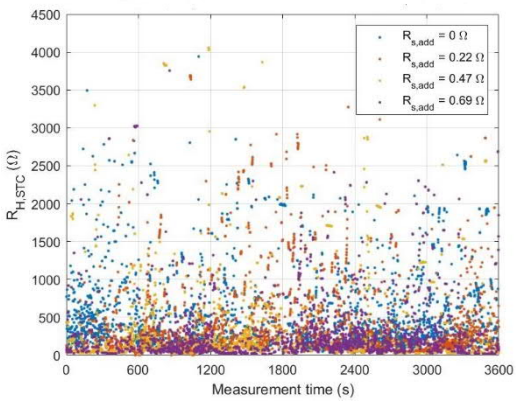

Figure 11: Experimental shunt resistance values converted to STC against the measurement time for different values of additional series resistance.

The photocurrent levels obtained via Eq. (10) from the measurements are provided in Fig. 12. As expected, the behavior is very similar to the one in Fig. 10. This is also in line with the common approximation $I_{ph} = I_{sc}$.

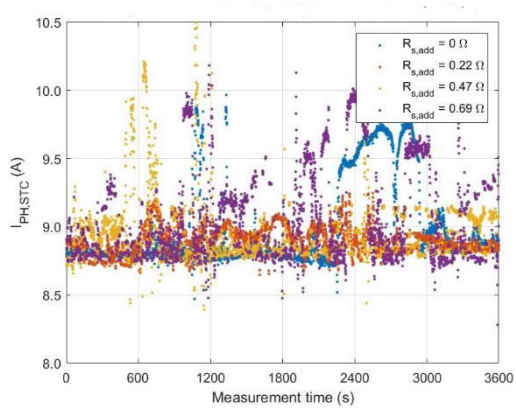

Figure 12: Photocurrent values converted from the experimental data to STC against the measurement time for different values of additional series resistance.

The final converted parameter under investigation is the saturation current which is shown in Fig. 13 for the studied *I-U* measurements. The peaks caused by irradiance changes are also visible in Fig. 13. A likely reason for the peaking is the previously mentioned inaccuracy of the one diode model at low irradiance levels but also the approximation of the open circuit voltage by using only the temperature dependent Eq. (12) might have an impact on this behavior. One possibility would be to replace Eq. (11) for the saturation current by the temperature and band gap dependent formula from [12]. However, this parameter is not a main interest on aging detection point of view.

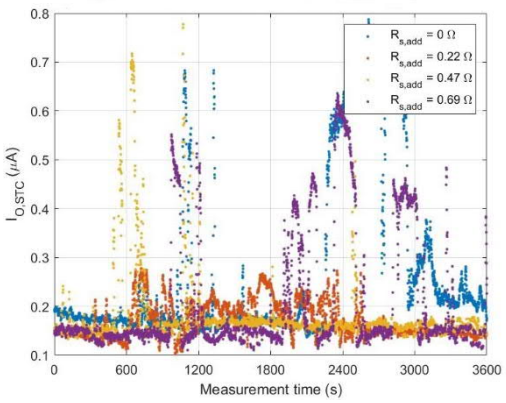

Figure 13: Saturation currents calculated from the experimental data and converted to STC against the measurement time for different levels of additional series resistance.

5 CONCLUSIONS

In this paper, detection of series resistance from measured PV panel *I-U* curves has been under investigation. Firstly, the relation between the measured voltage characteristics and the series resistance of a PV panel under different environmental conditions were studied and compared with corresponding simulations using the single diode model of the PV panel. The experimentally obtained parameter values were in overall agreement with the simulation results providing quite similar results, for example, for the U_{mpp}/U_{OC} ratio as a function of series resistance. It was also demonstrated that the used reverse Villalva procedure for converting single diode model parameter from the measured PV panel *I-U* curves to STC conditions works in good agreement with the procedure applied earlier by other author utilizing the Lambert W function. The conversion approach of the PV panel series resistance gave promising results especially at high irradiance levels for developing a real-time monitoring method for PV panel and system aging detection. In addition the conversion of other single diode model parameters from the measured *I-U* curves back to the reference STC conditions was demonstrated to be feasibly.

References

[1] G. Petrone, C. Ramos-Paja, G. Spagnuolo, Photovoltaic Sources Modeling, John Wiley & Sons Ltd (2017).
[2] G. Spagnuolo, K. Lappalainen, S. Valkealahti, P. Manganiello, 7th International Conference on Clean Electrical Power, Otranto, Italy, (2019).
[3] G. Spagnuolo, K. Lappalainen, S. Valkealahti, P. Manganiello, 13th IEEE PES PowerTech Conference, Milan, Italy, (2019).
[4] S. Cannizzaro, M. Di Piazza, M. Luna, G. Vitale, IEEE 23rd International Symposium on Industrial Electronics (2014) 2266.
[5] J. Bastidas-Rodriguez, E. Franco, G. Petrone, C. Ramos-Paja, G. Spagnuolo, Mathematics and Computers in Simulation, Vol. 131 (2017) 101.
[6] A. Faba, S. Gaiotto, G. Lozito, Solar Energy, Vol. 158 (2017) 520.
[7] A. Laudani, F. Fulginei, A. Salvini, Solar Energy, Vol. 108 (2014) 432.

[8] M. Villalva, J. Gazoli, E. Filho, IEEE Transactions on Power Electronics, Vol. 24 (2009) 1198.
[9] A. Elkholy, A. Abou El-Ela, Heliyon, Vol. 5 (2019).
[10] W. King, D. Boyson, J. Kratochvill, Sandia National Laboratories (2004).
[11] B. Marion, S. Rummel, A. Anderberg, Progress in Photovoltaics: Research and Applications, Vol. 12 (8) (2004) 593.
[12] W. De Soto, S. Klein, W. Beckman, Solar Energy, Vol. 80 (1) (2006) 78.
[13] V. Lo Brano, A. Orioli, G. Ciulla, A. Di Gangi, Solar Energy Materials and Solar Cells, Vol. 94 (8) (2010) 1358.
[14] D.Sera, R. Teodorescu, P. Rodriguez, 34th Annual Conference of IEEE Industrial Electronics (2008) 2195.
[15] J. Phang, D. Chan, J. Phillips, Electronics Letters, Vol. 20 (10) (1984) 406.
[16] G. Walker, Journal of Electrical and Electronics Engineering, Vol. 21 (1) (2001) 49.
[17] D. Torres Lobera, A. Mäki, J. Huusari, K. Lappalainen, T. Suntio, S. Valkealahti, International Journal of Photoenergy, Vol. 2013 (2013).